

SUPER-RESOLUTION ANALYSIS WITH MACHINE LEARNING FOR LOW-RESOLUTION FLOW DATA

Kai Fukami

Mechanical Engineering, Keio University, Yokohama, 223-8522, Japan
Mechanical Engineering, Florida State University, Tallahassee, FL 32310, USA
Mechanical and Aerospace Engineering, University of California, Los Angeles, CA 90095, USA
kai.fukami@keio.jp

Koji Fukagata

Mechanical Engineering, Keio University, Yokohama, 223-8522, Japan
fukagata@mech.keio.ac.jp

Kunihiko Taira

Mechanical and Aerospace Engineering, University of California, Los Angeles, CA 90095, USA
Mechanical Engineering, Florida State University, Tallahassee, FL 32310, USA
ktaira@seas.ucla.edu

ABSTRACT

Machine-learned super-resolution is performed to reconstruct the high-resolution flow (HR) field from low-resolution (LR) fluid flow data. As preliminary tests, we use two-dimensional cylinder and NACA0012 airfoil wake flow fields and observe good agreement with reference HR data. Next, we apply two machine-learned architectures based on the convolutional neural network (CNN) for two-dimensional decaying isotropic turbulence. The HR data sets are obtained from direct numerical simulation (DNS) and LR data sets are generated by max and average pooling operations. In this work, we present the hybrid Down-sampled Skip-Connection Multi-Scale (DSC/MS) model, which can reconstruct the flow field accurately from coarse input flow field data. Towards the end of the paper, we discuss the possibility of a machine-learned model for super-resolution in experimental and computational fluid dynamics.

INTRODUCTION

In recent years, the application of machine learning to fluid dynamics has shown success in turbulence modeling (Ling et al., 2016), reduced order modeling (San and Maulik, 2018), and turbulent inflow generation (Fukami et al., 2018a). In addition, these studies have shown the power of machine learning in extracting key features from tremendously big data generated from the high-dimensional complex flow systems (Kutz, 2016). In the present study, we use this strength of machine learning for reconstructing the high resolution flow field from the coarse flow data, known as 'super-resolution.'

To date, estimation and reconstruction of turbulent flow fields have been tackled experimentally and numerically. Chevalier et al. (2006) attempted to predict the characteristics of the main channel flow from the wall information using Kalman filter and extended-Kalman filter. Linear stochastic estimation is also applied to estimate the flow field in channel flow (Suzuki and Hasegawa, 2017) and

boundary layer (Marusic et al., 2010). Although these approaches show the applicability for turbulent flow systems, there remains challenges caused by strong nonlinearity and chaotic nature of turbulence.

The demand of data reconstruction is seen not only in fluid dynamics but also in computer science. In particular, example-based super resolution which can make a high-resolution signal from low-resolution signal, has been recognized as a strong method in image tasks (Salvador, 2017). Moreover, machine-learned super-resolution has emerged for image reconstruction and showed remarkable ability in recent years (Dong et al., 2016). With those recent advancements, we consider to apply the image-based concept for super-resolution analysis of turbulent flows.

Here, we propose a machine-learning based super-resolution analysis to reconstruct highly resolved turbulent flow fields using LR data. First, we consider two-dimensional cylinder and NACA0012 airfoil wake flows as preliminary study. Next, the convolutional neural network (CNN)-based architectures are applied to two-dimensional decaying isotropic turbulence. At the end of paper, we briefly discuss the possibility of machine-learned super-resolution analysis to experimental and computational fluid dynamics.

MACHINE LEARNING

In machine learning (ML), the nonlinear regression function \mathcal{F} are defined between the input data \mathbf{x} and desired output data \mathbf{y} such that $\mathbf{y} = \mathcal{F}(\mathbf{x}; \mathbf{w})$ with \mathbf{w} being the weight of the machine-learned model. In this work, we prepare the LR/HR data sets as \mathbf{x} and \mathbf{y} , respectively. In other words, the objective of the learning process in the current problem is to seek the optimized weight \mathbf{w} for obtaining desired output \mathbf{y} such that $\mathbf{w} = \operatorname{argmin}_{\mathbf{w}} \|\mathbf{y} - \mathcal{F}(\mathbf{x}; \mathbf{w})\|_2^2$, where we use the L_2 norm to optimize \mathbf{w} .

In present study, convolutional neural network (CNN)-based architectures are used to form \mathcal{F} (LeCun et al., 1998). CNN is one of the most widely used neural networks in the

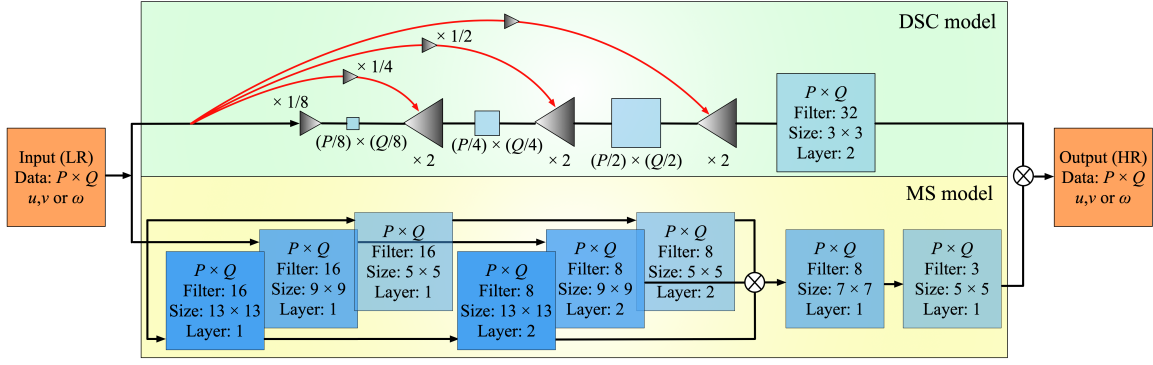


Figure 1. Schematic of the hybrid downsampled skip-connection multi-scale (DSC/MS) model.

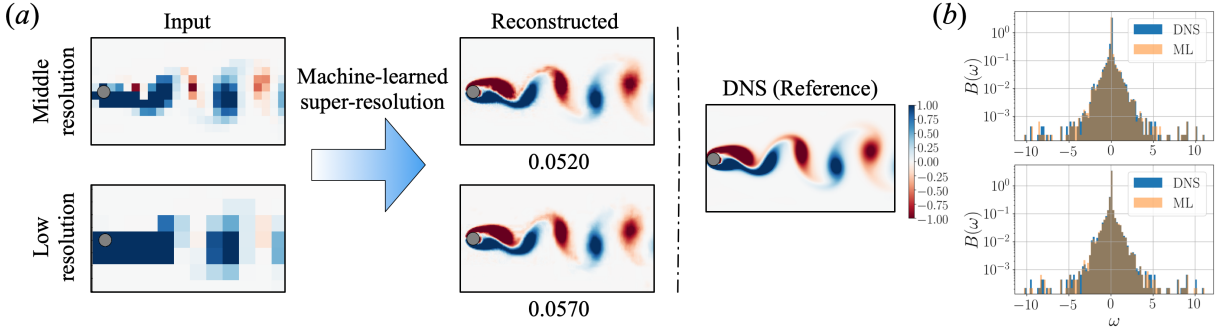


Figure 2. Super-resolution reconstruction of laminar cylinder wake at $Re_D = 100$. (a) The color contour of vorticity field ω . (b) Probability density function of vorticity field.

machine-learned super-resolution analysis of image tasks (Romano et al., 2017). In CNN, we consider the feature map called filter as the weight \mathbf{w} to extract the key feature between input data set and desired output data set. In addition, we propose a new network architecture for improving the reconstruction of image-based super resolution method for complex flows.

The CNN-based hybrid architecture shown in figure 1 is constructed by combining the downsampled skip-connection (DSC) model and multi-scale (MS) model. In DSC model, firstly $P \times Q$ pixel input data is compressed to $(P/8) \times (Q/8)$ pixels and entered to the machine learning model as shown in the green part of figure 1. The compression of the input data is known as an effective method for increasing the robustness against movement/rotation (Le et al., 2010). Next, we apply the skip-connection method (red arrows in figure 1) to avoid the overfitting which is often observed in deep CNN models. The DSC model tries to enhance the ability of the model against the large-scale structure of flow data by repeating the compression and skip-connection. We also combine the MS model proposed by Du et al. (2018) to predict the small-scale structures as illustrated by the yellow part of figure 1. According to their research, the use of various sizes of the feature map enhances the capability to catch in detail of image super-resolution. In this paper, we also use 5×5 , 9×9 and 13×13 filters following their work. At last, the outputs of DSC and MS model are merged, constructing the high-resolution flow field from the low-resolution data.

EXAMPLE 1: TWO-DIMENSIONAL CYLINDER FLOW

At first, let us demonstrate the machine-learned super-resolution analysis on the two-dimensional cylinder flow. The training data set is obtained from a two-dimensional direct numerical simulation (DNS) at $Re_D = 100$ (Taira and Colonius, 2007; Colonius and Taira, 2008). The governing equations are the incompressible Navier-Stokes equations,

$$\nabla \cdot \mathbf{u} = 0, \quad (1)$$

$$\frac{\partial \mathbf{u}}{\partial t} = -\mathbf{u} \cdot \nabla \mathbf{u} - \nabla p + \frac{1}{Re_D} \nabla^2 \mathbf{u}, \quad (2)$$

where \mathbf{u} , p and Re_D are the non-dimensionalized velocity vector, pressure and Reynolds number, respectively. The size of computational domain, the number of grid points and the range of time-steps are $(x/D, y/D) = [-0.7, 15] \times [-5, 5]$, $(N_x, N_y) = (192, 112)$ and $\Delta t = 2.50 \times 10^{-3}$. As the input and output attributes, we choose the vorticity field ω . In the present study, we adopt max and average pooling operations for obtaining the low-resolution data $((P/R) \times (Q/S))$ pixels. These operations are widely used in image processing. The max pooling is used to enhance the range of color and brightness. With the average pooling, we can extract the average value in over an arbitrary area.

In the first preliminary study of a cylinder wake, the max pooling operation with $R = S = 8$ (medium resolution) and $R = S = 16$ (low resolution) are used. Note that we also use the average pooling and $R = S = 32$ (super-low resolution) for turbulent flows in super-resolution analysis, as discussed later. In all trials in our paper, we use 70 % of the data set for training and the remaining 30 % for validation.

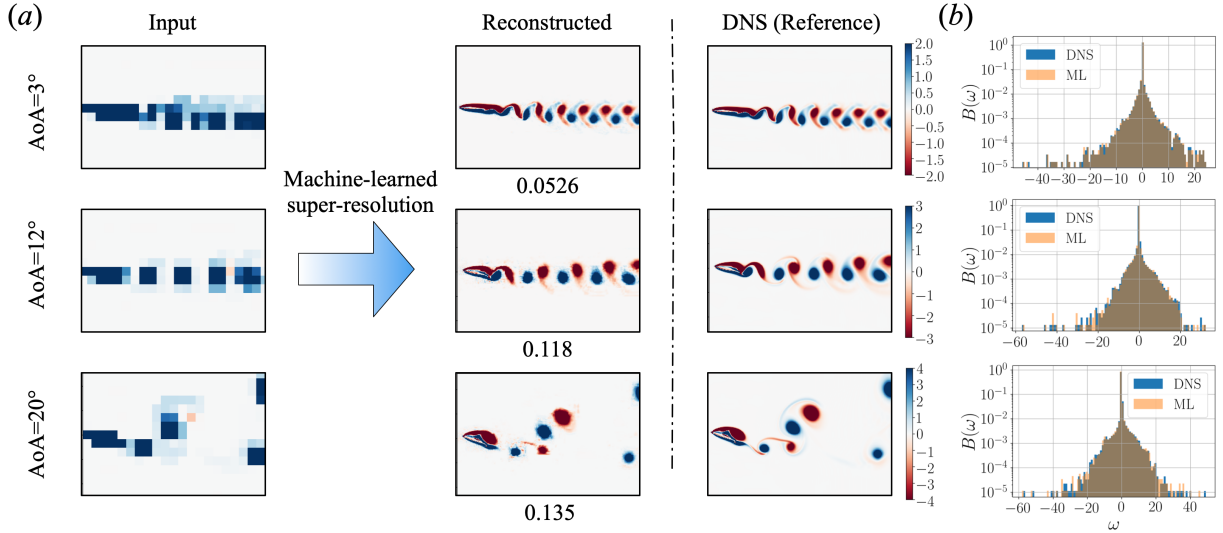


Figure 3. Super-resolution reconstruction of flow over a NACA0012 with a Gurney flap at $Re_c = 1000$. (a) The color contour of vorticity field ω . (b) Probability density function of the vorticity field.

To avoid that the ML model from lacking the generality for adopting only training data sets (i.e., overfitting), the early stopping criteria (Prechelt, 1998) is applied.

The procedure of machine-learned super-resolution analysis of the laminar cylinder wake is summarized in figure 2. Using our methodology, the vorticity field can be reconstructed from very coarse data with middle and low resolutions, as shown in figure 2(a). We also show the L_2 norm error, from low-resolution data $\varepsilon = \|\mathbf{x}^{\text{HR}} - \mathcal{F}(\mathbf{x})\|_2 / \|\mathbf{x}^{\text{HR}}\|_2$, below the color contours. The accuracy of the reconstructed flow field is lower than the middle resolution data because of the fidelity of coarse input data. We also confirm similar tendency in probability density function of vorticity field $B(\omega)$ shown in figure 2(b). From these observations, we verify the effectiveness of machine-learned super-resolution analysis for laminar flow.

EXAMPLE 2: TWO-DIMENSIONAL NACA0012 AIRFOIL WITH A GURNEY FLAP

In this section, we tackle a more complicated problem than the cylinder wake flow. The two-dimensional flow over a NACA0012 airfoil with a Gurney flap is considered (Gopalakrishnan Meena et al., 2018). The training data set is obtained by two-dimensional direct numerical simulation at $Re_c = 1000$. The size of computational domain, the number of grid points and the size of time step are $(x/c, y/c) = [-0.5, 7] \times [-2.5, 2.5]$, $(N_x, N_y) = (360, 240)$ and $\Delta t = 1.00 \times 10^{-3}$, respectively. We also use the vorticity field ω as input and output attributes. With the Gurney flap attached to the airfoil, we can observe various types wakes depending on the angles of attack α and the Gurney-flap height h/c . In what follows, we focus on cases with $h/c = 0.1$ and $\alpha = 3^\circ, 12^\circ$ and 20° to examine three characteristic wake regimes, as shown in figure 3. As the sub-sampled method, we use the max pooling with $R = S = 16$ (low resolution).

The super-resolution analysis for NACA0012 airfoil is shown in figure 3. Reconstructed vorticity fields are reasonable agreement with reference DNS data. In the same way with cylinder wake, we provide the L_2 norm error rate ε below the color contour in figure 3(a). It can be seen that the

error norm increases with the angles of attack α . This trend corresponds to the increasing unsteadiness in the wakes. Here, we note that this L_2 norm error rate is strict measurement without regard to similarity in translation or rotation. It means that error even if the L_2 norm appears high, ML based technique may still exhibit good agreement. In fact, the flow field can be reproduced and show reasonable agreement with reference data by machine-learned super-resolution technique, as shown in figure 3. For the example of airfoil wake with large unsteadiness, we also observe the capability of image based super-resolution analysis to reconstruct the flow from very coarse data.

EXAMPLE 3: TWO-DIMENSIONAL DECAYING ISOTROPIC TURBULENCE

To demonstrate machine-learned super-resolution analysis on turbulent flows, we consider the two-dimensional decaying isotropic turbulence. The flow field is obtained from a bi-periodic Fourier spectral incompressible two-dimensional direct numerical simulation (Taira et al. 2016). The reference DNS flow field is governed by two-dimensional vorticity transport equation

$$\frac{\partial \omega}{\partial t} + \mathbf{u} \cdot \nabla \omega = \frac{1}{Re} \nabla^2 \omega, \quad (3)$$

where $\mathbf{u} = (u, v)$ and ω are the velocity and vorticity variables. The size of computational domain and the number of grid points are $(L_x, L_y) = (1, 1)$ and $(N_x, N_y) = (128, 128)$, respectively. The Reynolds number Re is defined as $Re \equiv u^* l^* / \nu$, where u^* is the characteristic velocity based on the square root of the spatially averaged initial kinetic energy, l^* is the initial integral length, and ν is the kinematic viscosity. In our study, the 2D turbulent flows are computed with the initial Reynolds number $Re(t_0) = 74.6$ and $\Delta t = 1.950 \times 10^{-4}$. The max and average pooling operations are utilized with $R = S = 8$ (medium resolution), $R = S = 16$ (low resolution) and $R = S = 32$ (super-low resolution) to prepare the low-resolution data set. Here, we use the velocity component u as the input and output attributes.

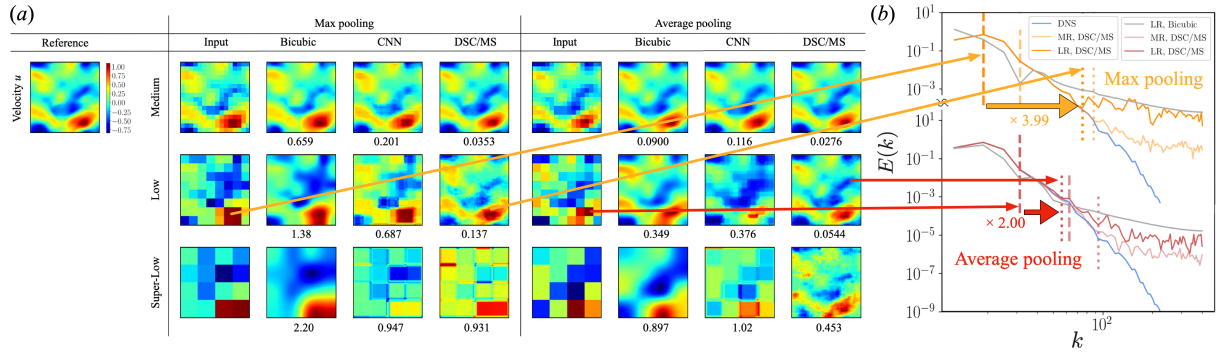


Figure 4. (a) The color contour of velocity field u from max and average pooled data., (b) Kinetic energy spectrum of medium and low resolution data. Dashed and dotted lines are k_{cutoff} and k_{max} .

The reconstructed turbulent flow fields from the coarse input data are summarized in figure 4(a). We compare 3 reconstruction methods: the bicubic interpolation, convolutional neural network and hybrid DSC/MS model. The bicubic interpolation is known as one of the traditional super-resolution techniques, based on the filter operation (Keys, 1981). The L_2 error norms are indicated underneath the color contours.

With the simple bicubic interpolation, the reconstructed flow fields from the max and average pooled medium resolution data show reasonable agreement with reference DNS data. However, the accuracy of reconstruction by the bicubic interpolation decreases with the fidelity of input coarse data, as shown in figure 4(a). It can be seen that the bicubic interpolation simply smoothes the flow field. In particular, we can observe this tendency in super-low resolution results.

As the first trial using machine-learned super-resolution for turbulent flows, we use a 3-layer convolutional neural network. Based on the max pooled data, the L_2 error norms are in general lower with the machine learning techniques, compared to the results from the bicubic interpolation. However, the returned reconstructed flow fields from low and super-low resolution data are pixelized. Furthermore, the CNN reconstructions does not show an advantage against simple bicubic interpolation, as shown in figure 4(a). Thus, we consider an improved network architecture for taking the multi-scale of turbulent flows account into machine-learned super-resolution analysis.

The hybrid DSC/MS model is adopted to enhance the results of machine-learned super-resolution analysis. In all cases, the L_2 error norms are lowered with the hybrid DSC/MS model. In the low-resolution ($R = S = 8$) data sets of both pooling methods, the flow fields are reconstructed compared to the bicubic interpolation and CNN. Moreover, we observe further advantage with the hybrid DSC/MS model. See the average pooled super-low resolution data in figure 4(a). The hybrid DSC/MS model can recover flow structures as well as the reference DNS data from very coarse input data on 4×4 grid. From these observation, we confirm the remarkable strength of the hybrid DSC/MS model for super-resolution in turbulent flows.

Let us assess the reconstructed kinetic energy spectra over the spatial wave number k . The energy spectrum computed by max and averaged pooled medium and low resolution reconstructed fields using the hybrid DSC/MS model are shown in figure 4(b). The dashed and dotted lines are k_{cutoff} of the coarse input data and k_{max} of reconstructed

data, respectively. The maximum wave number k_{max} is defined where the kinetic energy spectra of reference DNS and reconstructed data matches up to 90%. It can be seen that the k_{max} are recovered by super-resolution reconstruction. The recovery ratio $k_{\text{max}}/k_{\text{cutoff}}$ based on max and average pooled low-resolution data are approximately 4 and 2, respectively. The difference of the recovery ratio between the max and average pooling inputs is influenced by the initial error level, as shown in figures 4(a) and (b). Although not shown, similar results are obtained for the velocity v flow field and energy spectra. From these results, we find that proposed machine-learned model is effective in providing the super-resolution data for turbulent flows.

For further details on the case of using the vorticity field ω as input/output attribute and the dependence of the number of the training snapshot data n_{snapshot} , we refer the readers to Fukami et al. (2018b).

CONCLUSION

We proposed a machine-learned super-resolution analysis approach for reconstructing flow fields. Two-dimensional cylinder wake and NACA0012 airfoil wake were considered as laminar flow examples. The proposed hybrid DSC/MS model was found to reconstruct the flow structures and the probability density function well. In the grossly coarse input data for the two-dimensional turbulent flow, the DSC/MS model was able to recover the flow field on 128×128 image from on input data with as little as 4×4 pixels. The capability of present model was also shown in the energy spectra profile. As future analysis, extensions to three-dimensional flows and the parameter-tuning of machine learning models can be considered. Moreover, we plan to apply the machine-learned super-resolution method to the analysis of PIV measurements and LES (subgrid-scale) modeling.

ACKNOWLEDGEMENTS

Kai Fukami and Koji Fukagata are supported by the Japan Society for the Promotion of Science (KAKENHI grant number: 18H03758). Kunihiko Taira acknowledges support from ARO (grant number: W911NF-17-1-0118) and AFOSR (grant number: FA9550-16-1-0650).

REFERENCES

Ling, J., Kurzwski, A., and Templeton, J., 2016, Reynolds averaged turbulence modelling using deep neural

networks with embedded invariance, *Journal of Fluid Mechanics*, Vol. 807, pp. 155-166.

San, O., and Maulik, R., 2018, Extreme learning machine for reduced order modeling of turbulent geophysical flows, *Physical Review E*, vol. 97(042322)

Fukami, K., Kawai, K., and Fukagata, K., 2018a, A synthetic turbulent inflow generator using machine learning, in review, *Physical Review Fluids*, available on arXiv, arXiv:1806.08903 [physics.flu-dyn]

Kutz, J., N., 2016, Deep learning in fluid dynamics, *Journal of Fluid Mechanics*, Vol. 814, pp. 1-4.

Chevalier, M., Hœpffner, J., Bewley, T., R., and Henningson, D., S., 2006, "State estimation in wall-bounded flow systems. Part 2. Turbulent flows", *Journal of Fluid Mechanics*, Vol. 552, pp. 167-187.

Suzuki, T., and Hasegawa, Y., 2017, "Estimation of turbulent channel flow at $Re_\tau = 100$ based on the wall measurement using a simple sequential approach", *Journal of Fluid Mechanics*, Vol. 830, pp. 760-796.

Marusic, I., Mathis, R., and Hutchins, N., 2010, Predictive Model for Wall-Bounded Turbulent Flow, *Science*, Vol. 329 (5988), pp. 193-196.

Salvador, J., 2017, Example-based Super Resolution, Elsevier Academic Press.

Dong, C., Loy, C., C., He, K. and Tang, X., 2016, Image super-resolution using deep convolutional networks, *IEEE Transactions on Pattern Analysis and Machine Intelligence*, Vol. 38(2), pp. 295-307.

LeCun, Y., Bottou, L., Bengio, Y., and Haffner, P., 1998, Gradient-based learning applied to document recognition, *Proc. IEEE*, Vol. 86 (11), 2278

Romano, Y., Ishidoro, J. and Milanfar, P., 2017, RAISR: rapid and accurate image super resolution. *IEEE Transactions Computational Imaging* vol. 3(1), pp. 110-125.

Le, Q., Ngiam, J., Chen, Z., Chia, D., H., and Koh, P., 2010, Tiled convolutional neural networks, *Advances in*

Neural Information Processing Systems, vol. 23, pp. 1279-1287.

Du, X., Qu, X., He, Y., and Guo, D., 2018, Single Image Super-Resolution Based on Multi-Scale Competitive Convolutional Neural Network, *Sensors*, Vol. 18 (789), pp. 1-17.

Taira, K., and Colonius, T., 2007, The immersed boundary method: A projection approach. *Journal of Computational Physics*, vol. 225(2), pp. 2118-2137.

Colonius, T., and Taira, K., 2008, A fast immersed boundary method using a nullspace approach and multi-domain far-field boundary conditions. *Computer Methods in Applied Mechanics and Engineering*, vol. 197, pp. 2131-2146.

Prechelt, L., 1998, Automatic early stopping using cross validation: quantifying the criteria, *Neural Networks*, Vol. 11 (4), pp. 761-767.

Gopalakrishnan Meena, M., Taira, K., and Asai, K., 2018, Airfoil Wake Modification with Gurney Flap at Low-Reynolds Number, *AIAA Journal*, vol. 56(4), pp. 1348-1359.

Kurtulus, D., F., 2015, On the unsteady behavior of the flow around NACA 0012 airfoil with steady external conditions at $Re = 1000$, *International Journal of Micro Air Vehicles*, Vol. 7(3), pp. 301-326.

Taira, K., Nair, G., A., and Brunton, S., L., 2016, Network structure of two-dimensional decaying isotropic turbulence, *Journal of Fluid Mechanics*, Vol. 795, R2, pp. 1-11.

Keys, R., 1981, Cubic convolution interpolation for digital image processing. *IEEE Transactions on Acoustics, Speech, and Signal Processing*, vol. 29(6), pp. 1153-1160.

Fukami, K., Fukagata, K., and Taira, K., 2018b, Super-resolution reconstruction of turbulent flows with machine learning, in review, *Journal of Fluid Mechanics*, available on arXiv, arXiv:1811.11328 [physics.flu-dyn]